Distributed null-steering beamforming for wireless sensor networks

Keyvan Zarifi*†, Sofiene Affes*, and Ali Ghrayeb†
*Université du Québec, INRS-EMT, 800, de la Gauchetière west, Montreal, QC, H5A 1K6, Canada
{zarifi,affes}@emt.inrs.ca
†Concordia University, 1455 de Maisonneuve west, Montreal, QC, H3G 1M8, Canada
aghrayeb@ece.concordia.ca

***Abstract*— Null-steering transmit beamformers aim to maximize the received signal power at the direction of the access point (AP) while inflicting minimal interfering effect on unintended receivers. However, existing null-steering beamformers may not be directly applied to wireless sensor networks (WSNs) as they require every node to be aware of the locations of other nodes in the network.**

In this paper, a novel null-steering beamformer is introduced that can be implemented in uniformly distributed WSNs in which each node is oblivious of other nodes' locations. The average beampattern expression of the proposed beamformer is derived and its properties are analytically studied. In particular, it is shown that the average beampattern of the proposed beamformer is similar to that of the conventional beamformer in directions with far angular distance from any unintended receiver. The analytical results are also adopted to design a null-steering beamformer with a single null and required average beampattern properties. The optimal null position is obtained which minimizes the maximum sidelobe of the average beampattern while having negligible deteriorating effect on the received power at the AP. Finally, computer simulations are used to validate the analytical results as well as to confirm the effectiveness of the design approach.

I. Introduction

Distributed beamforming for wireless sensor networks (WSNs) has recently been introduced [1]-[4] as a means of establishing an energy-efficient and reliable communication link between small battery-powered sensor nodes and an access point (AP) that is typically located far beyond the transmission range of each individual node. This goal is achieved by having the nodes simultaneously transmit properly weighted versions of a common message such that their transmitted signals are coherently combined at the AP. As such, the nodes aggregate transmission range is substantially increased in the direction of the AP without requiring to amplify their total transmission power.

In many practical scenarios, not only is it required to increase the received power at the AP, but also it is crucial to avoid inducing any interfering effect to unintended receivers. Proposed for centralized antenna arrays, the null-steering beamformer [5]-[7] additionally fulfills the latter task by setting the antenna transmission weights such that while the transmitted signals are being coherently combined at the AP, their superposition approaches zero in the directions of unintended receivers.

Unfortunately, the null-steering beamformer may not be directly applied in WSNs as it requires that the exact locations of all nodes to be globally available at every node; a requirement that does not conform with the distributed nature of WSNs and, furthermore, is not scalable as the number of nodes grows large.

In this paper, we assume that the nodes are uniformly distributed on a disc of arbitrary radius [1], [8]-[10] and use this statistical knowledge to introduce a novel null-steering beamformer that can be applied to WSNs in which each node is oblivious of all other nodes' locations. The average beampattern expression of the proposed beamformer is obtained and it is further proved that, as the number of nodes grows, every arbitrary realization of the beampattern converges to the average beampattern with probability one. It is shown that the average gain of the proposed null-steering beamformer is approximately equal to that of the conventional beamformer [1] in directions with an angular distance far enough from any unintended receiver while being inversely proportional to the number of nodes in the directions of the unintended receivers.

It is shown that, in the absence of any unintended receiver, the null positions may be treated as design parameters that can be adjusted to form an average beampattern with sidelobe peaks considerably smaller than those of the average beampattern of the conventional beamformer [1]. In particular, a null-steering beamformer is designed whose single null is optimally positioned to minimize the maximum sidelobe of the average beampattern while inducing a negligible received power degradation at the AP.

The rest of the paper is organized as follows. Section II presents the signal model and Section III proposes the distributed null-steering beamformer. Properties of the average beampattern of the proposed null-steering beamformer are discussed in Section IV and a single-null null-steering beamformer is designed in Section V. The concluding remarks are given in Section VI.

Notation: Uppercase and lowercase bold letters denote matrices and vectors, respectively. $[\cdot]_{il}$, $[\cdot]_{\cdot,l}$, and $[\cdot]_i$ are the (i,l)-th entry of a matrix, l-th column of a matrix, and i-th entry of a vector, respectively. $j \triangleq \sqrt{-1}$, $\mathbf{I}$ is the identity matrix, and $\mathbf{e}_i$ is a vector with one in the i-th position and zeros elsewhere. $(\cdot)^T$ and $(\cdot)^H$ denote the transpose and the Hermitian transpose, respectively. $\|\cdot\|$ is the 2-norm of a vector and $|\cdot|$ is the absolute value. $\mathrm{E}\{\cdot\}$ stands for the statistical expectation and $(\xrightarrow{ep1})$ $\xrightarrow{p1}$ denotes (element-wise) convergence with probability one. $J_n(\cdot)$ stands for the n-th order Bessel function of the first kind.

978-1-4244-4148-8/09/$25.00 ©2009
This full text paper was peer reviewed at the direction of IEEE Communications Society subject matter experts for publication in the IEEE "GLOBECOM" 2009 proceedings.

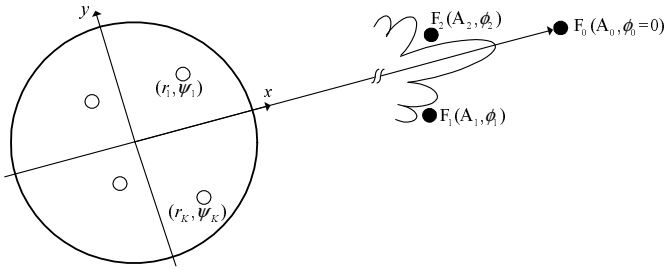

Fig. 1. $\tilde{P}(\phi)$ (dB) versus ϕ (deg) for $K = 200$.

II. System Model

The geometrical structure of the WSN cluster and the receiver terminals are illustrated in Fig. 1 where K cluster nodes are uniformly distributed on $D(O, R)$, the disc centered at O with an arbitrary radius R [1], [8]-[10], while the cluster AP as well as L unintended receivers are located in the same plane containing $D(O, R)$. The cluster nodes form a virtual antenna array and collaboratively transmit a common message $z(t)$ aiming to simultaneously achieve the following two goals:

- **G1:** The received signal power at the AP is maximized.
- **G2:** The received signal powers at all unintended receivers are zero.

Without any loss of generality, let O be the pole and the line connecting O to the AP be the x-axis of a polar coordinate system. Denote the polar coordinates of the k-th cluster node as (r_k, ψ_k) and the polar coordinates of the AP and the unintended receivers as $(A_0, \phi_0 = 0)$ and $(A_l, \phi_l),\ l = 1, \ldots, L$, respectively. The following assumptions are adopted throughout this paper:

- **A1:** The AP as well as all unintended receivers are in the far-field of the WSN cluster such that

$$A_l \gg R \qquad l = 0, 1, \ldots, L. \tag{1}$$

  As such, the signals transmitted from any two arbitrary cluster nodes and received at one of the above terminals have equal path losses.
- **A2:** The bandwidth of $z(t)$ is narrow enough such that $z(t)$ is almost constant during $2R/c$ seconds where c is the speed of an electromagnetic wave.
- **A3:** There is no signal reflection or scattering and, therefore, no multipath fading or shadowing.
- **A4:** The k-th node is only aware of its own coordinates (r_k, ψ_k) and the directions of the receiving terminals $\phi_l,\ l = 0, 1, \ldots, L$, while being unaware of the locations of all other nodes as well as $A_l,\ l = 0, 1, \ldots, L$.

Assumptions **A1**-**A3** are common in the literature of array processing for planar waves while **A4** is due to the distributed and unsupervised characteristics of WSNs.

Let

$$s_k(t) = w_k z(t) e^{-j2\pi ft} \tag{2}$$

denote the transmitted signal from the k-th node where $z(t)$ is the modulating signal with $\xi_z = \mathrm{E}\{|z(t)|^2\}$, w_k is the k-th node transmission weight, and f is the carrier frequency. Using **A1**-**A3**, it can be shown that the received signal at an arbitrary point $F_\bullet(A_\bullet, \phi_\bullet)$ in the far-field due to the k-th node transmission is given by

$$y_{F_\bullet,k}(t) = \beta_{F_\bullet} \chi(t, A_\bullet) w_k e^{-j\frac{2\pi}{\lambda} r_k \cos(\phi_\bullet - \psi_k)} e^{-j2\pi ft} \tag{3}$$

where $\chi(t, A_\bullet) \triangleq e^{j\frac{2\pi}{\lambda}A_\bullet} z\left(t - \frac{A_\bullet}{c}\right)$. Let us introduce

$$\mathbf{a}_{\phi_\bullet} \triangleq [e^{j\frac{2\pi}{\lambda} r_1 \cos(\phi_\bullet - \psi_1)} \ \ldots \ e^{j\frac{2\pi}{\lambda} r_K \cos(\phi_\bullet - \psi_K)}]^T \tag{4}$$

$$\mathbf{w} \triangleq [w_1 \ \ldots \ w_K]^T. \tag{5}$$

The total received signal at $F_\bullet$ due to all cluster nodes can be represented as

$$y_{F_\bullet}(t) = \beta_{F_\bullet} \chi(t, A_\bullet) e^{-j2\pi ft} \mathbf{a}_{\phi_\bullet}^H \mathbf{w}. \tag{6}$$

As such, the total received power at $F_\bullet$ is equal to

$$\xi_{F_\bullet} = \beta_{F_\bullet}^2 \xi_z |\mathbf{a}_{\phi_\bullet}^H \mathbf{w}|^2. \tag{7}$$

Let $\mathbf{A} \triangleq [\mathbf{a}_{\phi_1} \ \ldots \ \mathbf{a}_{\phi_L}]$. It is direct to observe that **G1** and **G2** can be achieved if $\mathbf{w}$ is a solution to

$$\max_{\mathbf{w}} |\mathbf{a}_0^H \mathbf{w}|^2 \qquad \text{s.t.} \qquad \mathbf{A}^H \mathbf{w} = \mathbf{0}. \tag{8}$$

The solution to (8) is given by [5], [6]

$$\mathbf{w}_{\mathrm{ns}} = (\mathbf{I} - \mathbf{P}_{\mathbf{A}})\, \mathbf{a}_0 \tag{9}$$

where $\mathbf{P}_{\mathbf{A}} \triangleq \mathbf{A}(\mathbf{A}^H\mathbf{A})^{-1}\mathbf{A}^H$ is the projection matrix onto the subspace spanned by the columns of $\mathbf{A}$. In the array processing literature, the solution to (8) is sometimes called the null-steering beamformer [5], [7]. This justifies the subscript of $\mathbf{w}_{\mathrm{ns}}$ as well as the title of this manuscript.

III. Distributed Null-Steering Beamformer

Let us define

$$\mathbf{E} \triangleq \frac{1}{K}\mathbf{A}^H\mathbf{A}, \qquad \mathbf{g}_{\phi_\bullet} \triangleq \frac{1}{K}\mathbf{A}^H\mathbf{a}_{\phi_\bullet} \tag{10}$$

and

$$\mathbf{d} \triangleq \mathbf{E}^{-1}\mathbf{g}_0. \tag{11}$$

The null-steering beamformer (9) can be alternatively rewritten as

$$\mathbf{w}_{\mathrm{ns}} = \mathbf{a}_0 - \mathbf{A}\mathbf{d}. \tag{12}$$

Equation (12) shows that **G1** and **G2** are simultaneously achieved if we have for $k = 1, \ldots, K$ that

$$\begin{aligned} w_k = [\mathbf{w}_{\mathrm{ns}}]_k &= [\mathbf{a}_0]_k - \sum_{i=1}^{L} [\mathbf{A}]_{ki}[\mathbf{d}]_i \\ &= e^{j\frac{2\pi}{\lambda} r_k \cos(\phi_0 - \psi_k)} - \sum_{i=1}^{L} e^{j\frac{2\pi}{\lambda} r_k \cos(\phi_i - \psi_k)} [\mathbf{d}]_i. \end{aligned} \tag{13}$$

Note from (13) that the null-steering beamformer (12) can be implemented only when the k-th node ($k = 1, \ldots, K$) knows all $e^{j\frac{2\pi}{\lambda} r_k \cos(\phi_i - \psi_k)}$ for $i = 0, \ldots, L$ as well as all entries of $\mathbf{d}$. It follows from **A4** that the k-th node can use its available knowledge to obtain $e^{j\frac{2\pi}{\lambda} r_k \cos(\phi_i - \psi_k)},\ i = 0, \ldots, L$. However, this knowledge is not sufficient to obtain $[\mathbf{d}]_1, \ldots, [\mathbf{d}]_L$. In fact, it is straightforward to verify that $[\mathbf{d}]_i, i = 1, \ldots, L$ depend on the locations of all nodes in the cluster. Therefore, $\mathbf{w}_{\mathrm{ns}}$ can be implemented only if every

978-1-4244-4148-8/09/$25.00 ©2009
This full text paper was peer reviewed at the direction of IEEE Communications Society subject matter experts for publication in the IEEE "GLOBECOM" 2009 proceedings.

node knows the exact locations of all nodes in the cluster. Unfortunately, this requirement does not conform with **A4**.

To get around this problem and be able to implement (an approximate) null-steering beamformer in a distributed fashion, one needs to substitute $\mathbf{d}$ in (12) with an approximating vector whose entries depend only on the parameters *commonly* known at every node, that is, $\phi_l,\ l = 0, 1, \ldots, L$. In light of the fact that a WSN node usually has a limited nonrenewable energy resource, it makes practical sense to use a large number of nodes in the collaborative beamforming in return to a low transmission power from each individual node. For scenarios with a large K, $\lim_{K\to\infty}\mathbf{d}$ can serve as an accurate approximation of $\mathbf{d}$. However, to be able to use $\lim_{K\to\infty}\mathbf{d}$ in lieu of $\mathbf{d}$, we require to verify that $\lim_{K\to\infty}\mathbf{d}$ only depends on $\phi_l,\ l = 0, 1, \ldots, L$.

Note from (11) that $\mathbf{d} = \mathbf{E}^{-1}\mathbf{g}_0$ where, according to (10),

$$[\mathbf{E}]_{mn} = \frac{1}{K}\mathbf{a}_{\phi_m}^H \mathbf{a}_{\phi_n} \tag{14}$$

$$[\mathbf{g}_0]_m = \frac{1}{K}\mathbf{a}_{\phi_m}^H \mathbf{a}_0. \tag{15}$$

Equations (14) and (15) show that $\lim_{K\to\infty}\mathbf{d}$ is entirely dependent on $\lim_{K\to\infty}\frac{1}{K}\mathbf{a}_{\phi_m}^H\mathbf{a}_{\phi_n},\ m = 1, \ldots, L,\ n = 0, 1, \ldots, L$. The following theorem on asymptotic properties of $\frac{1}{K}\mathbf{a}_{\phi_m}^H\mathbf{a}_{\phi_n}$ is essential in our later developments.

Theorem 1: Consider $\mathbf{a}_{\phi_\bullet}$ as defined in (4). Assuming that the nodes are uniformly distributed on $D(O, R)$, we have

$$\frac{1}{K}\mathbf{a}_{\phi_m}^H\mathbf{a}_{\phi_n} = \frac{1}{K}\sum_{k=1}^{K} e^{j\alpha(\phi_n-\phi_m)z_k} \tag{16}$$

where $\tilde{R} \triangleq R/\lambda$ and $\alpha(\phi_\bullet) \triangleq 4\pi\tilde{R}\sin\left(\frac{\phi_\bullet}{2}\right)$. Moreover,

$$z_k \triangleq \frac{r_k}{R}\cdot\sin\left(\psi_k - \frac{\phi_n+\phi_m}{2}\right) \qquad k = 1, \ldots, K \tag{17}$$

are independent and identically distributed (i.i.d.) random variables with the following probability density function (PDF):

$$f_{z_k}(z) = \frac{2}{\pi}\sqrt{1-z^2} \qquad z_k \in [-1, 1]. \tag{18}$$

We have for $m \neq n$ that

$$\begin{aligned}\frac{1}{K}\mathrm{E}\left\{\mathbf{a}_{\phi_m}^H\mathbf{a}_{\phi_n}\right\} &= \mathrm{E}\left\{e^{j\alpha(\phi_n-\phi_m)z_k}\right\}\\ &= \frac{2J_1\left(\alpha(\phi_n-\phi_m)\right)}{\alpha(\phi_n-\phi_m)}\end{aligned} \tag{19}$$

and

$$\begin{aligned}\lim_{K\to\infty}\frac{1}{K}\mathbf{a}_{\phi_m}^H\mathbf{a}_{\phi_n} &\xrightarrow{p1} \frac{1}{K}\sum_{k=1}^{K}\mathrm{E}\left\{e^{j\alpha(\phi_n-\phi_m)z_k}\right\}\\ &= \frac{2J_1\left(\alpha(\phi_n-\phi_m)\right)}{\alpha(\phi_n-\phi_m)}.\end{aligned} \tag{20}$$

The proof of Theorem 1 as well as those of our later results are presented in [11].

Using (20) in (14) and (15), we obtain the following result.

Corollary 1: Consider the $L \times L$ matrix $\bar{\mathbf{E}}$ and the $L \times 1$ vector $\bar{\mathbf{g}}_0$ with

$$[\bar{\mathbf{E}}]_{mn} \triangleq \begin{cases}\frac{2}{\alpha(\phi_n-\phi_m)}J_1\left(\alpha(\phi_n-\phi_m)\right) & m \neq n\\ 1 & m = n\end{cases} \tag{21}$$

$$[\bar{\mathbf{g}}_0]_m \triangleq \frac{2}{\alpha(\phi_m)}J_1\left(\alpha(\phi_m)\right). \tag{22}$$

We have

$$\lim_{K\to\infty}\mathbf{E} \xrightarrow{ep1} \bar{\mathbf{E}}, \qquad \lim_{K\to\infty}\mathbf{g}_0 \xrightarrow{ep1} \bar{\mathbf{g}}_0. \tag{23}$$

Moreover,

$$\lim_{K\to\infty}\mathbf{d} \xrightarrow{ep1} \bar{\mathbf{d}} \tag{24}$$

where

$$\bar{\mathbf{d}} \triangleq \bar{\mathbf{E}}^{-1}\bar{\mathbf{g}}_0. \tag{25}$$

Corollary 1 shows that the entries of $\lim_{K\to\infty}\mathbf{d}$ converge with probability one to limiting values that exclusively depend on $\alpha(\phi_n-\phi_m),\ m = 1, \ldots, L,\ n = 0, 1 \ldots, L$. As $\alpha(\phi_n-\phi_m)$ depends solely on $\phi_n-\phi_m$, it follows that $\phi_l,\ l = 0, 1, \ldots, L$ are sufficient to determine the entries of $\lim_{K\to\infty}\mathbf{d}$. Therefore, we propose to use

$$\bar{\mathbf{w}}_{\mathrm{ns}} = \mathbf{a}_0 - \mathbf{A}\bar{\mathbf{d}} \tag{26}$$

in lieu of $\mathbf{w}_{\mathrm{ns}}$. Note that $\bar{\mathbf{w}}_{\mathrm{ns}}$ accurately approximates the null-steering beamformer $\mathbf{w}_{\mathrm{ns}}$ for a large K, and, in addition, it can be implemented in a distributed fashion.

Assume that $\bar{\mathbf{w}}_{\mathrm{ns}}$ is used in the WSN cluster. As follows from (7), the far-field received signal power in an arbitrary direction $\phi_\bullet$ is proportional to

$$P(\phi_\bullet|\mathbf{z}) \triangleq \frac{1}{K^2}\left|\mathbf{a}_{\phi_\bullet}^H\bar{\mathbf{w}}_{\mathrm{ns}}\right|^2. \tag{27}$$

$P(\phi_\bullet|\mathbf{z})$ is called the far-field beampattern and $\mathbf{z} \triangleq [z_1, \ldots, z_K]$ is used in (27) to stress the fact that $P(\phi_\bullet|\mathbf{z})$ is a random variable that depends on the entries of $\mathbf{z}$. As $P(\phi_\bullet|\mathbf{z})$ is a function of $\mathbf{z}$, the study of the average beampattern

$$\tilde{P}(\phi_\bullet) \triangleq \mathrm{E}_{\mathbf{z}}\left\{P(\phi_\bullet|\mathbf{z})\right\} \tag{28}$$

is of significant importance. Section IV investigates the properties of $\tilde{P}(\phi_\bullet)$ and proves that as the number of nodes K grows large, $P(\phi_\bullet|\mathbf{z})$ converges to $\tilde{P}(\phi_\bullet)$ for any arbitrary realization of $\mathbf{z}$. This further justifies the practical importance of $\tilde{P}(\phi_\bullet)$.

IV. Properties of the Average Beampattern

A. Average Beampattern Expression

The main result of this section is given in the following theorem.

Theorem 2: Assuming that the approximate null-steering beamformer (26) is used, we have

$$\begin{aligned}\tilde{P}(\phi_\bullet) = &\frac{1}{K}\left(1 - \bar{\mathbf{g}}_0^T\bar{\mathbf{E}}^{-1}\bar{\mathbf{g}}_0\right) +\\ &\left(1-\frac{1}{K}\right)\left(\frac{2}{\alpha(\phi_\bullet)}J_1\left(\alpha(\phi_\bullet)\right) - \bar{\mathbf{g}}_0^T\bar{\mathbf{E}}^{-1}\bar{\mathbf{g}}_{\phi_\bullet}\right)^2\end{aligned} \tag{29}$$

978-1-4244-4148-8/09/$25.00 ©2009

where $\bar{\mathbf{g}}_{\phi_\bullet}$ is an $L \times 1$ vector with

$$[\bar{\mathbf{g}}_{\phi_\bullet}]_l \triangleq \begin{cases} \frac{2}{\alpha(\phi_\bullet - \phi_l)} J_1\left(\alpha(\phi_\bullet - \phi_l)\right) & \phi_\bullet \neq \phi_l \\ 1 & \phi_\bullet = \phi_l \end{cases}. \quad (30)$$

moreover, it holds for any arbitrary realization of $\mathbf{z}$ that

$$\lim_{K\to\infty} P(\phi_\bullet|\mathbf{z}) \xrightarrow{p1} \lim_{K\to\infty} \tilde{P}(\phi_\bullet) = \left(\frac{2}{\alpha(\phi_\bullet)} J_1\left(\alpha(\phi_\bullet)\right) - \bar{\mathbf{g}}_0^T \bar{\mathbf{E}}^{-1} \bar{\mathbf{g}}_{\phi_\bullet}\right)^2. \quad (31)$$

As can be observed from (29), $\tilde{P}(\phi_\bullet)$ is comprised of two terms: 1) The first term that is independent of $\phi_\bullet$ and is nonnegative (see Subsection IV-C) but diminishes to zero as K grows large. This term determines the floor level of the average beampattern curve; 2) The second term that depends on $\phi_\bullet$, is nonnegative, and does not converge to zero as K grows large. This term determines the shape of the average beampattern curve. In particular, the maximum points of this term are the peak points of the average beampattern sidelobe. We further call the roots of this term as the "nulls" of the average beampattern (see [1] for a similar nomenclature). The following discussions on the properties of $\tilde{P}(\phi_\bullet)$ are also in order.

B. Average Beampattern at ϕ_l

To examine the effectiveness of $\bar{\mathbf{w}}_{\rm ns}$ in reducing the received signal power at $\phi_l,\ l = 1, \ldots, L$, let us obtain

$$\tilde{P}(\phi_l) = \frac{1}{K}\left(1 - \bar{\mathbf{g}}_0^T \bar{\mathbf{E}}^{-1} \bar{\mathbf{g}}_0\right) + \left(1 - \frac{1}{K}\right)\left(\frac{2}{\alpha(\phi_l)} J_1\left(\alpha(\phi_l)\right) - \bar{\mathbf{g}}_0^T \bar{\mathbf{E}}^{-1} \bar{\mathbf{g}}_l\right)^2. \quad (32)$$

Note from (21) and (30) that $\bar{\mathbf{g}}_l = \bar{\mathbf{E}}_{\cdot,l} = \bar{\mathbf{E}}\mathbf{e}_l$. It directly follows from the latter equality that the second term in the right-hand side (RHS) of (32) is equal to zero and we have

$$\tilde{P}(\phi_l) = \frac{1}{K}\left(1 - \bar{\mathbf{g}}_0^T \bar{\mathbf{E}}^{-1} \bar{\mathbf{g}}_0\right) \quad (33)$$

for $l = 1, \ldots, L$. Equation (33) shows that $\phi_l,\ l = 1, \ldots, L$, are in fact the nulls of the average beampattern. It can also be observed from the latter equation that the price of using $\bar{\mathbf{w}}_{\rm ns}$ is lieu of $\mathbf{w}_{\rm ns}$ is to elevate the null levels at $\phi_l,\ l = 1, \ldots, L$ from zero to the RHS of (33). Note that, as K grows large, $\bar{\mathbf{w}}_{\rm ns}$ converges to $\mathbf{w}_{\rm ns}$ and the RHS of (33) converges to zero.

C. Average Beampattern at the Direction of the AP

Using the fact that $\lim_{\phi_\bullet \to 0} 2J_1(\alpha(\phi_\bullet))/\alpha(\phi_\bullet) = 1$ in (29), we have

$$\tilde{P}(0) = \left(1 - \bar{\mathbf{g}}_0^T \bar{\mathbf{E}}^{-1} \bar{\mathbf{g}}_0\right)^2 + \frac{1}{K} \bar{\mathbf{g}}_0^T \bar{\mathbf{E}}^{-1} \bar{\mathbf{g}}_0 \left(1 - \bar{\mathbf{g}}_0^T \bar{\mathbf{E}}^{-1} \bar{\mathbf{g}}_0\right). \quad (34)$$

Equation (34) shows that $\tilde{P}(0)$ entirely depends on K and $\bar{\mathbf{g}}_0^T \bar{\mathbf{E}}^{-1} \bar{\mathbf{g}}_0$. It can be observed from (10) and (23) as well as the definition of $\mathbf{P}_{\mathbf{A}}$ that

$$\lim_{K\to\infty} \frac{1}{K} \left\|\mathbf{P}_{\mathbf{A}} \mathbf{a}_0\right\|^2 \xrightarrow{p1} \bar{\mathbf{g}}_0^T \bar{\mathbf{E}}^{-1} \bar{\mathbf{g}}_0. \quad (35)$$

As $\|\mathbf{P}_{\mathbf{A}} \mathbf{a}_0\|$ is the length of the orthogonal projection of $\mathbf{a}_0$ onto the column span of $\mathbf{A}$, we have $\|\mathbf{P}_{\mathbf{A}} \mathbf{a}_0\| \leq \|\mathbf{a}_0\|$, and, therefore,

$$0 \leq \frac{1}{K} \left\|\mathbf{P}_{\mathbf{A}} \mathbf{a}_0\right\|^2 \leq 1 \quad (36)$$

where the left-hand side (LHS) inequality holds with equality if $\mathbf{a}_0$ is orthogonal to the column span of $\mathbf{A}$ and the RHS inequality holds with equality if $\mathbf{a}_0$ is in the column span of $\mathbf{A}$. It follows from (35) and (36) that $\bar{\mathbf{g}}_0^T \bar{\mathbf{E}}^{-1} \bar{\mathbf{g}}_0 \in [0, 1]$. Note from (34) that $\tilde{P}(0)$ is a decreasing function of $\bar{\mathbf{g}}_0^T \bar{\mathbf{E}}^{-1} \bar{\mathbf{g}}_0$ in the latter interval and, as $\bar{\mathbf{g}}_0^T \bar{\mathbf{E}}^{-1} \bar{\mathbf{g}}_0$ increases from 0 to 1, $\tilde{P}(0)$ decreases from 1 to 0. It should be mentioned that the decrease in $\tilde{P}(0)$ is the price that may have to be paid for devising nulls in the directions of unintended receivers. In fact, as $\bar{\mathbf{w}}_{\rm ns}$ is derived such that $|\mathbf{a}_{\phi_l}^H \bar{\mathbf{w}}_{\rm ns}| \approx 0,\ l = 1, \ldots, L$, the more $\mathbf{a}_0$ leans towards the column span of $\mathbf{A}$, the smaller the $|\mathbf{a}_0^H \bar{\mathbf{w}}_{\rm ns}|$, and, consequently, the more the decrease in $\tilde{P}(0)$. Note that a similar property also holds for the null-steering beamformer in the array processing literature. We show in Subsection IV-E that, under a mild condition, $\bar{\mathbf{g}}_0^T \bar{\mathbf{E}}^{-1} \bar{\mathbf{g}}_0 \approx 0$ and therefore suppressing the received signal power in the directions of unintended receivers has a negligible impact on $\tilde{P}(0)$.

D. Average Beampattern for $L = 0$

When there is no unintended receiver, that is, $L = 0$, $\bar{\mathbf{w}}_{\rm ns}$ reduces to the conventional beamformer

$$\mathbf{w}_{\rm c} = \mathbf{a}_0 \quad (37)$$

and $\tilde{P}(\phi_\bullet)$ in (29) boils down to

$$\tilde{P}_{\rm c}(\phi_\bullet) = \frac{1}{K} + \left(1 - \frac{1}{K}\right)\left(\frac{2}{\alpha(\phi_\bullet)} J_1\left(\alpha(\phi_\bullet)\right)\right)^2. \quad (38)$$

The same expression as in (38) has been obtained before in [1] for the conventional scenario in which the AP is the only receiving terminal. As can be observed from (38), the beamformer gain at the origin achieves its maximal possible value and we have

$$\tilde{P}_{\rm c}(0) = 1. \quad (39)$$

Due to the oscillatory shape of $J_1(x)$, $\tilde{P}_{\rm c}(\phi_\bullet)$ has infinite number of sidelobe nulls and peaks. Let $\tilde{\phi}_{\rm n,c}^{(n)}$ and $\nu^{(n)}$ denote the n-th sidelobe null of $\tilde{P}_{\rm c}(\phi_\bullet)$ and the n-th positive root of $J_1(x)$, respectively. From (38) we have $\alpha(\tilde{\phi}_{\rm n,c}^{(n)}) = \nu^{(n)}$ and, therefore,

$$\tilde{\phi}_{\rm n,c}^{(n)} = 2 \arcsin\left(\frac{\nu^{(n)}}{4\pi\tilde{R}}\right). \quad (40)$$

Let us also denote the n-th sidelobe peak point of $\tilde{P}_{\rm c}(\phi_\bullet)$ by $\tilde{\phi}_{\rm p,c}^{(n)}$. Simple approximations of $\tilde{\phi}_{\rm n,c}^{(n)}$ and $\tilde{\phi}_{\rm p,c}^{(n)}$ can be obtained if one uses

$$J_1(x) \approx \sqrt{\frac{2}{\pi x}} \cos\left(x - \frac{3\pi}{4}\right) \qquad x \gg 1 \quad (41)$$

in (38) and simplifies the average beampattern expression to [1]

$$\tilde{P}_{\rm c}(\phi_\bullet) \approx \frac{1}{K} + \left(1 - \frac{1}{K}\right) \frac{8}{\pi \alpha(\phi_\bullet)^3} \cos^2\left(\alpha(\phi_\bullet) - \frac{3\pi}{4}\right). \quad (42)$$

978-1-4244-4148-8/09/$25.00 ©2009

It can be shown from (42) that if $\tilde{R}$ is large enough such that $\alpha(\phi_\bullet) \triangleq 4\pi\tilde{R}\sin(\phi_\bullet/2) \gg 1$, then [1]

$$\tilde{\phi}_{\mathrm{n,c}}^{(n)} \approx 2\arcsin\left(\frac{n+1/4}{4\tilde{R}}\right) \tag{43}$$

$$\tilde{\phi}_{\mathrm{p,c}}^{(n)} \approx 2\arcsin\left(\frac{n+3/4}{4\tilde{R}}\right) \tag{44}$$

It also follows from (42) and (44) that [1]

$$\tilde{P}_{\mathrm{c}}(\tilde{\phi}_{\mathrm{p,c}}^{(n)}) \approx \frac{1}{K} + \left(1-\frac{1}{K}\right)\cdot\frac{1}{\pi}\left(\frac{2}{\pi(n+3/4)}\right)^3. \tag{45}$$

Note from (45) that the n-th sidelobe peak of $\tilde{P}_{\mathrm{c}}(\phi_\bullet)$ is independent of $\tilde{R}$ and is almost proportional to $1/n^3$.

E. Approximate Average Beampattern for $\alpha(\phi_l) \gg 1$

Note from (22) that as $\alpha(\phi_l)$ increases, $[\bar{\mathbf{g}}_0]_l$ converges to zero. In particular, when the angular distances between the AP and the unintended receivers are not very small and $\tilde{R}$ is large enough such that

$$\alpha(\phi_l) = 4\pi\tilde{R}\sin\left(\frac{\phi_l}{2}\right) \gg 1 \qquad l = 1,\ldots,L, \tag{46}$$

then (41) can be used in (22) to obtain

$$[\bar{\mathbf{g}}_0]_l \approx \frac{1}{\sqrt{\pi}}\cdot\left(\frac{2}{\alpha(\phi_l)}\right)^{\frac{3}{2}}\cos\left(\alpha(\phi_l)-\frac{3\pi}{4}\right). \tag{47}$$

As such, when (46) holds, we have that $\bar{\mathbf{g}}_0^T\bar{\mathbf{E}}^{-1}\bar{\mathbf{g}}_0 \ll 1$. Using the latter inequality in (29), it follows that

$$\tilde{P}(\phi_\bullet) \approx \frac{1}{K} + \left(1-\frac{1}{K}\right)\left(\frac{2}{\alpha(\phi_\bullet)}J_1\left(\alpha(\phi_\bullet)\right) - \bar{\mathbf{g}}_0^T\bar{\mathbf{E}}^{-1}\bar{\mathbf{g}}_{\phi_\bullet}\right)^2. \tag{48}$$

A direct result of (48) is that

$$\tilde{P}(0) \approx \frac{1}{K} + \left(1-\frac{1}{K}\right)\left(1-\bar{\mathbf{g}}_0^T\bar{\mathbf{E}}^{-1}\bar{\mathbf{g}}_0\right)^2 \approx 1. \tag{49}$$

Approximation (49) shows that if (46) holds, then $\tilde{P}(0)$ approaches its maximal value. In such a case, suppressing the power in the directions of the unintended receivers does not inflict a noticeable decrease in the received power at the AP.

Approximation (48) can be further simplified if $\phi_\bullet$ is not in a close proximity of any $\phi_l,\ l = 1,\ldots,L$. In fact, if $|\phi_\bullet - \phi_1|,\ldots,|\phi_\bullet-\phi_L|$ are large enough such that

$$|\alpha(\phi_\bullet-\phi_l)| = 4\pi\tilde{R}\sin\left(\frac{|\phi_\bullet-\phi_l|}{2}\right) \gg 1 \qquad l = 1,\ldots,L, \tag{50}$$

then

$$[\bar{\mathbf{g}}_{\phi_\bullet}]_l \approx \frac{1}{\sqrt{\pi}}\left(\frac{2}{|\alpha(\phi_\bullet-\phi_l)|}\right)^{\frac{3}{2}}\cos\left(|\alpha(\phi_\bullet-\phi_l)|-\frac{3\pi}{4}\right). \tag{51}$$

In such a case, it follows from (47) and (51) that $|\bar{\mathbf{g}}_0^T\bar{\mathbf{E}}^{-1}\bar{\mathbf{g}}_{\phi_\bullet}| \ll |2J_1(\alpha(\phi_\bullet))/\alpha(\phi_\bullet)|$ and

$$\tilde{P}(\phi_\bullet) \approx \frac{1}{K} + \left(1-\frac{1}{K}\right)\left(\frac{2}{\alpha(\phi_\bullet)}J_1\left(\alpha(\phi_\bullet)\right)\right)^2 = \tilde{P}_{\mathrm{c}}(\phi_\bullet). \tag{52}$$

Equation (52) states that if (46) holds and $\phi_\bullet$ is not close to the direction of any of the unintended receivers, then $P(\phi_\bullet)$ is approximately equal to the average beampattern of the conventional beamformer. Note that if (46) holds and $\phi_\bullet = \phi_l$, then (33) yields

$$\tilde{P}(\phi_l) = \frac{1}{K}\left(1-\bar{\mathbf{g}}_0^T\bar{\mathbf{E}}^{-1}\bar{\mathbf{g}}_0\right) \approx \frac{1}{K}. \tag{53}$$

The discussion of this subsection can be summarized as follows: Assume that (46) holds. Then, $\tilde{P}(\phi_\bullet)$ looks similar to $\tilde{P}_{\mathrm{c}}(\phi_\bullet)$ for all $\phi_\bullet$ far enough from any $\phi_1,\ldots,\phi_L$. In particular, $\tilde{P}(\phi_\bullet)$ and $\tilde{P}_{\mathrm{c}}(\phi_\bullet)$ have similar sets of nulls and peaks in the angular intervals that are not close to any $\phi_1,\ldots,\phi_L$. Note that $\tilde{P}(\phi_\bullet)$ has additional nulls at $\phi_1,\ldots,\phi_L$ and when $\phi_\bullet$ is close to a ϕ_l, (48) (and not (52)) is a reliable approximation of $\tilde{P}(\phi_\bullet)$.

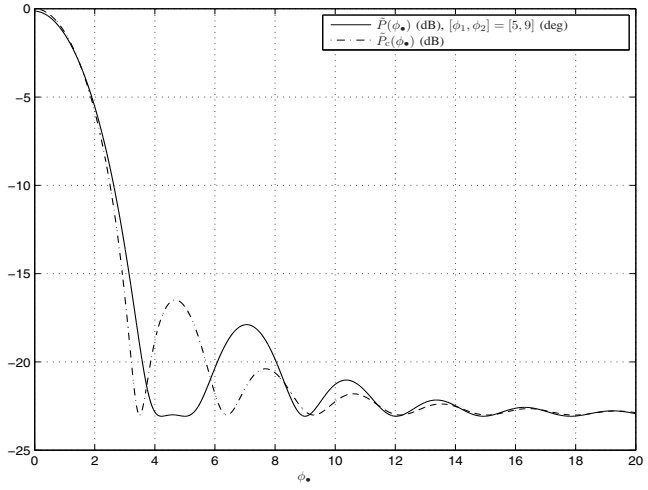

Fig. 2. $\tilde{P}(\phi_\bullet)$ and $\tilde{P}_{\mathrm{c}}(\phi_\bullet)$ versus $\phi_\bullet$. Two unintended receivers at $[\phi_1,\phi_2] = [5,9]$ (deg) are considered.

Fig. 2 displays $\tilde{P}(\phi_\bullet)$ versus $\phi_\bullet$ for $[\phi_1,\phi_2] = [5,9]$ (deg). For the sake of comparison, $\tilde{P}_{\mathrm{c}}(\phi_\bullet)$ is also plotted. Fig. 2 shows that two nulls of $\tilde{P}(\phi_\bullet)$ are exactly located at ϕ_1 and ϕ_2, and, moreover, as both aforementioned angles are far enough from $\phi_0 = 0$, we have that $\tilde{P}(0) \approx 1$. This figure also verifies that, increasing $\phi_\bullet - \phi_2$, $\tilde{P}(\phi_\bullet)$ tends to approach $\tilde{P}_{\mathrm{c}}(\phi_\bullet)$. The above observations corroborate our discussion in this subsection.

V. Null-steering beamformer design

As shown in Subsection IV-D (see also [1]), the sidelobe peaks of the conventional beamformer are fixed and cannot be reduced by, for instance, by adjusting $\tilde{R}$. This is an undesired property as, for instance, $\tilde{P}_{\mathrm{c}}(\tilde{\phi}_{\mathrm{p,c}}^{(1)})$, the most prominent sidelobe peak of $\tilde{P}_{\mathrm{c}}(\phi_\bullet)$, may be unacceptably large. In contrast to the conventional beamformer, the sidelobe peaks of the proposed null-steering beamformer are not fixed and depend on the null locations $\phi_1,\ldots,\phi_L$. Therefore, positioning nulls at proper locations, $\bar{\mathbf{w}}_{\mathrm{ns}}$ may alternatively be used to decrease the sidelobe peaks.

Let $\tilde{P}(\phi_\bullet,\phi_1)$ denote the average beampattern of a null-steering beamformer with a single null at ϕ_1. Note that the second argument is added to $\tilde{P}(\phi_\bullet,\phi_1)$ to stress that ϕ_1 is a design parameter. Let us also denote $\mathcal{A} \subseteq (0,\ \pi)$ such that

$$\tilde{P}(0,\phi_1) \geq 0.9 \qquad \forall\phi_1 \in \mathcal{A}. \tag{54}$$

978-1-4244-4148-8/09/$25.00 ©2009
This full text paper was peer reviewed at the direction of IEEE Communications Society subject matter experts for publication in the IEEE "GLOBECOM" 2009 proceedings.

Inequality (54) implies that selecting ϕ_1 from $\mathcal{A}$ guarantees that the decrease in the received power at the AP due to the use of $\bar{\mathbf{w}}_{\rm ns}$ is negligible. In what follows, we aim to find ϕ_1^* such that: 1) $\phi_1^* \in \mathcal{A}$; and 2) Among all $\phi_1 \in \mathcal{A}$, ϕ_1^* minimizes the largest sidelobe peak of $\tilde{P}(\phi_\bullet, \phi_1)$.

When $L = 1$, we have $\bar{\mathbf{g}}_{\phi_\bullet} = 2J_1(\alpha(\phi_\bullet - \phi_1))/\alpha(\phi_\bullet - \phi_1)$ for $\phi_\bullet \neq \phi_1$ and $\bar{\mathbf{E}} = 1$. Therefore, for $\phi_\bullet \neq \phi_1$, the average beampattern expression (29) reduces to

$$\tilde{P}(\phi_\bullet, \phi_1) = \frac{1}{K}\left(1 - \left(\frac{2J_1(\alpha(\phi_1))}{\alpha(\phi_1)}\right)^2\right) + \left[\left(1 - \frac{1}{K}\right) \times \left(\frac{2J_1\left(\alpha(\phi_\bullet)\right)}{\alpha(\phi_\bullet)} - \frac{2J_1(\alpha(\phi_1))}{\alpha(\phi_1)} \cdot \frac{2J_1(\alpha(\phi_\bullet - \phi_1))}{\alpha(\phi_\bullet - \phi_1)}\right)^2\right] \quad (55)$$

and, hence,

$$\tilde{P}(0, \phi_1) \geq \left(1 - \left(\frac{2J_1(\alpha(\phi_1))}{\alpha(\phi_1)}\right)^2\right)^2. \quad (56)$$

It is direct to show from (56) that

$$\mathcal{A} = \left[2\arcsin\left(\frac{3}{4\pi\tilde{R}}\right),\ \pi\right) \quad (57)$$

satisfies (54). Note from (57) that $\alpha(\phi_1^*) \geq 3$ and, further, for any $\phi_1 \in \mathcal{A}$ we have

$$\tilde{P}(\phi_\bullet, \phi_1) \approx \frac{1}{K} + \left(1 - \frac{1}{K}\right) \times \left(\frac{2J_1\left(\alpha(\phi_\bullet)\right)}{\alpha(\phi_\bullet)} - \frac{2J_1(\alpha(\phi_1))}{\alpha(\phi_1)} \cdot \frac{2J_1(\alpha(\phi_\bullet - \phi_1))}{\alpha(\phi_\bullet - \phi_1)}\right)^2 \quad (58)$$

Note that the RHS of (58) depends on $\alpha(\phi_1)$, $\alpha(\phi_\bullet)$, and $\alpha(\phi_\bullet - \phi_1)$ where

$$\begin{aligned}\alpha(\phi_\bullet - \phi_1) &= 4\pi\tilde{R}\sin\left(\frac{\phi_\bullet - \phi_1}{2}\right) \\ &= \alpha(\phi_\bullet)\cos\left(\frac{\phi_1}{2}\right) - \alpha(\phi_1)\cos\left(\frac{\phi_\bullet}{2}\right) \\ &= \alpha(\phi_\bullet)\sqrt{1 - \left(\frac{\alpha(\phi_1)}{4\pi\tilde{R}}\right)^2} - \\ &\qquad \alpha(\phi_1)\sqrt{1 - \left(\frac{\alpha(\phi_\bullet)}{4\pi\tilde{R}}\right)^2}. \end{aligned} \quad (59)$$

Using (59) in (58), it immediately follows that, in general, $\tilde{P}(\phi_\bullet, \phi_1)$ is a function of $\alpha(\phi_1)$, $\alpha(\phi_\bullet)$, and $\tilde{R}$. However, as will be argued below, if $\tilde{R} \geq 5$, then $\tilde{P}(\phi_\bullet, \phi_1)$ is almost independent of $\tilde{R}$ for the whole range of $\alpha(\phi_1)$ and $\alpha(\phi_\bullet)$ of our concern. To substantiate the above claim, let $\tilde{\phi}_{\rm p}^{(\star)}(\phi_1)$ denote the largest sidelobe peak point of $\tilde{P}(\phi_\bullet, \phi_1)$ for a given ϕ_1. The argument ϕ_1 in $\tilde{\phi}_{\rm p}^{(\star)}(\phi_1)$ is used to emphasize the fact that the largest sidelobe peak point of the average beampattern depends on ϕ_1. Moreover, note that, in contrary to the conventional beamformer, there is no guarantee that the first sidelobe peak of $\tilde{P}(\phi_\bullet, \phi_1)$ is its largest one. Therefore, the superscript $^{(\star)}$ (and not $^{(1)}$) is used to denote the index of the largest sidelobe peak of $\tilde{P}(\phi_\bullet, \phi_1)$. It has been shown in [11], and will be further verified here through computer simulations, both $\alpha(\phi_1^*)$ and $\alpha(\tilde{\phi}_{\rm p}^{(\star)}(\phi_1))$ should be smaller than $\nu^{(3)} = 10.1735$. The bounds on $\alpha(\phi_1^*)$ and $\alpha(\tilde{\phi}_{\rm p}^{(\star)}(\phi_1))$ suggest that, to find ϕ_1^* and $\tilde{\phi}_{\rm p}^{(\star)}(\phi_1)$, it is only required to search in the intervals corresponding to $\alpha(\phi_1) \in [3, \nu^{(3)}]$ and $\alpha(\phi_\bullet) \in [0, \nu^{(3)}]$. If $\tilde{R} \geq 5$, we have in the latter intervals that

$$\min\left\{\sqrt{1 - \left(\frac{\alpha(\phi_1)}{4\pi\tilde{R}}\right)^2}, \sqrt{1 - \left(\frac{\alpha(\phi_\bullet)}{4\pi\tilde{R}}\right)^2}\right\} = 0.9868. \quad (60)$$

Using (60) in (59), it holds for any $\tilde{R} \geq 5$, $\alpha(\phi_1) \in [3, \nu^{(3)}]$, and $\alpha(\phi_\bullet) \in [0, \nu^{(3)}]$ that $\alpha(\phi_\bullet - \phi_1) \approx \alpha(\phi_\bullet) - \alpha(\phi_1)$. The latter approximation shows that if $\tilde{R} \geq 5$ and $\alpha(\phi_1)$ and $\alpha(\phi_\bullet)$ are in the intervals of our concern, then $\tilde{P}(\phi_\bullet, \phi_1)$ is solely a function of two variables $\alpha(\phi_1)$ and $\alpha(\phi_\bullet)$ and can be equivalently represented as

$$\tilde{P}(\alpha(\phi_\bullet), \alpha(\phi_1)) = \frac{1}{K} + \left(1 - \frac{1}{K}\right) \times \left(\frac{2J_1\left(\alpha(\phi_\bullet)\right)}{\alpha(\phi_\bullet)} - \frac{2J_1(\alpha(\phi_1))}{\alpha(\phi_1)} \cdot \frac{2J_1(\alpha(\phi_\bullet) - \alpha(\phi_1))}{\alpha(\phi_\bullet) - \alpha(\phi_1)}\right)^2. \quad (61)$$

Approximation (61) not only represents the average beampattern expression as an explicit function of $\alpha(\phi_1)$ and $\alpha(\phi_\bullet)$, but also implies that, if $\tilde{R} \geq 5$, then $\alpha(\tilde{\phi}_{\rm p}^{(\star)}(\phi_1))$ and $\alpha(\phi_1^*)$ are independent of $\tilde{R}$. The latter result is of considerable practical importance, as it shows that if $\tilde{R} \geq 5$, then $\alpha(\phi_1^*)$ is globally optimal for any WSN cluster size.

To determine $\alpha(\phi_1^*)$, one can first use (61) to obtain $\alpha(\tilde{\phi}_{\rm p}^{(\star)}(\phi_1))$ for every $\alpha(\phi_1) \in [3, \nu^{(3)}]$. Then, we have that

$$\alpha(\phi_1^*) = \arg\min \tilde{P}\left(\alpha\left(\tilde{\phi}_{\rm p}^{(\star)}(\phi_1)\right), \alpha(\phi_1)\right) \quad (62)$$

among all $\alpha(\phi_1) \in [3, \nu^{(3)}]$.

Fig. 3 displays $\tilde{P}(\alpha(\tilde{\phi}_{\rm p}^{(\star)}(\phi_1)), \alpha(\phi_1))$ (dB) versus $\alpha(\phi_1)$ for $K \to \infty$. For the sake of comparison, $\tilde{P}_{\rm c}(\tilde{\phi}_{\rm p,c}^{(1)})$ is also shown with a dash-dotted line. Note from (61) that, unlike $\tilde{P}(\alpha(\tilde{\phi}_{\rm p}^{(\star)}(\phi_1)), \alpha(\phi_1))$, $\alpha(\tilde{\phi}_{\rm p}^{(\star)}(\phi_1))$ is independent of K. It should also be mentioned that the part of the curve of $\tilde{P}(\alpha(\tilde{\phi}_{\rm p}^{(\star)}(\phi_1)), \alpha(\phi_1))$ that is plotted with a bold line corresponds to those values of $\alpha(\phi_1)$ for which $\tilde{\phi}_{\rm p}^{(\star)}(\phi_1) =$

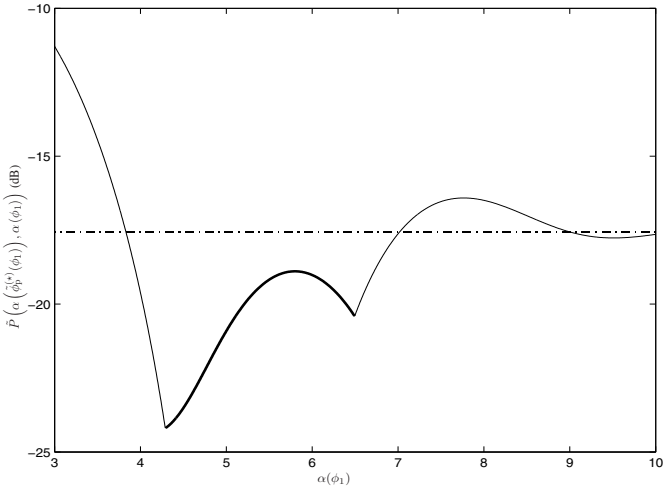

Fig. 3. $\tilde{P}(\alpha(\tilde{\phi}_{\rm p}^{(\star)}(\phi_1)), \alpha(\phi_1))$ (dB) versus $\alpha(\phi_1) \in [3, \nu^{(3)}]$ for $K \to \infty$.

978-1-4244-4148-8/09/$25.00 ©2009
This full text paper was peer reviewed at the direction of IEEE Communications Society subject matter experts for publication in the IEEE "GLOBECOM" 2009 proceedings.

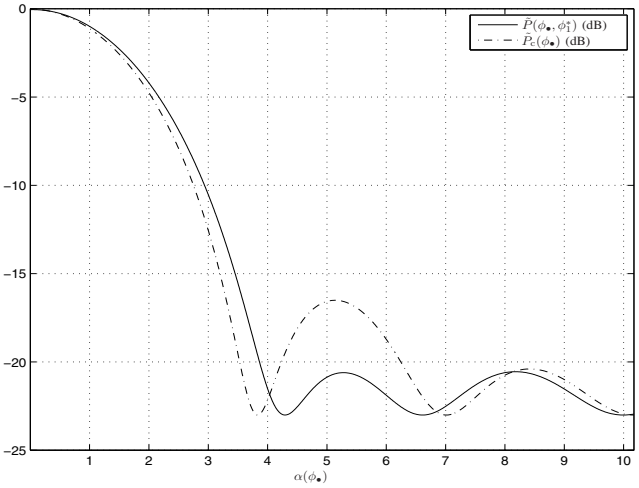

Fig. 4. $P(\phi_\bullet, \phi_1^*)$ and $P_{\rm c}(\phi_\bullet)$ versus $\alpha(\phi_\bullet)$.

$\tilde{\phi}_{\rm p}^{(2)}(\phi_1)$. We have $\tilde{\phi}_{\rm p}^{(\star)}(\phi_1) = \tilde{\phi}_{\rm p}^{(1)}(\phi_1)$ in other parts of the curve.

It can be observed from Fig. 3 that $\alpha(\phi_1^*) = 4.2950$. Fig. 3 also shows that if $\alpha(\phi_1^*)$ is selected, then the first and the second sidelobe peaks of the average beampattern are equal to each other but are larger than all other sidelobe peaks. We also have $\alpha(\tilde{\phi}_{\rm p}^{(1)}(\phi_1^*)) = 5.2776$ and $\alpha(\tilde{\phi}_{\rm p}^{(2)}(\phi_1^*)) = 8.1822$. Moreover, it holds for $K = \infty$ that

$$\Delta = 10\log_{10}\left(\frac{\tilde{P}_{\rm c}\left(\tilde{\phi}_{\rm p,c}^{(1)}\right)}{\tilde{P}\left(\alpha\left(\tilde{\phi}_{\rm p}^{(\star)}(\phi_1^*)\right), \alpha\left(\phi_1^*\right)\right)}\right) \approx 6.6. \quad (63)$$

Note that although $\alpha(\phi_1^*)$ and $\alpha(\tilde{\phi}_{\rm p}^{(\star)}(\phi_1^*))$ are independent of K, it is direct to show from (61) that Δ is a positive and increasing function of K. It should also be stressed that the so-obtained $\alpha(\phi_1^*)$ and $\alpha(\tilde{\phi}_{\rm p}^{(\star)}(\phi_1^*))$ confirm the validity of our selected upper-bounds.

The results of this section can be summarized as follows:

- Assume that $\tilde{R} \geq 5$ and $\bar{\mathbf{w}}_{\rm ns}$ with a single null is used to form a transmission beam towards the AP. Then, among all null locations that have negligible impact on the received power at the AP, the optimal null location that minimizes the largest sidelobe peak of $\tilde{P}(\phi_\bullet, \phi_1)$ is given by

$$\phi_1^* \approx 2\arcsin\left(\frac{4.2950}{4\pi\tilde{R}}\right). \quad (64)$$

  Positioning null at ϕ_1^*, the first and the second sidelobe peaks become equal and we have

$$\tilde{\phi}_{\rm p}^{(\star)}(\phi_1) = \tilde{\phi}_{\rm p}^{(1)}(\phi_1) \approx 2\arcsin\left(\frac{5.2776}{4\pi\tilde{R}}\right)$$
$$\tilde{\phi}_{\rm p}^{(\star)}(\phi_1) = \tilde{\phi}_{\rm p}^{(2)}(\phi_1) \approx 2\arcsin\left(\frac{8.1758}{4\pi\tilde{R}}\right). \quad (65)$$

  Moreover, if ϕ_1^* is used, then, depending on K, the resulting largest sidelobe peaks can be up to 6.6 (dB) less than the largest sidelobe peak of the conventional beamformer.

Fig. 4 shows $P(\phi_\bullet, \phi_1^*)$ in (58) versus $\alpha(\phi_\bullet)$ for $K = 200$. $P_{\rm c}(\phi_\bullet)$ is also displayed in this figure. As can be observed from Fig. 4, the first and the second sidelobe peaks of $P(\phi_\bullet, \phi_1^*)$ are equal and both are much smaller than the first sidelobe peak of $P_{\rm c}(\phi_\bullet)$. This validates the analytical results of this subsection and confirms the effectiveness of selecting ϕ_1^* as in (64) to reduce the sidelobe peaks of the average beampattern.

VI. Conclusions

A null-steering beamformer has been proposed that, in contrary to its existing counterparts, is applicable to WSNs wherein each node is unaware of other nodes' locations. Assuming that the nodes are uniformly distributed on a two-dimensional plane, the average beampattern expression of the proposed beamformer has been derived. It has been shown that the average gain of this beamformer is inversely proportional to the number of nodes at the directions of unintended receivers and is approximately equal to that of the conventional beamformer in directions with far angular distance from any unintended receiver.

A single-null null-steering beamformer has been considered and the optimal null position was obtained that minimizes the maximal level of the average beampattern sidelobe without causing a noticeable degradation in the received power at the AP.

References

[1] H. Ochiai, P. Mitran, H. V. Poor, and V. Tarokh, "Collaborative beamforming for distributed wireless ad hoc sensor networks," *IEEE Trans. Signal Process.,* vol. 53, pp. 4110-4124, Nov. 2005.

[2] R. Mudumbai, G. Barriac, U. Madhow, "On the feasibilty of distributed beamforming in wireless sensor networks," *IEEE Trans. Wirless Commun.,* vo. 6, pp. 1754-1763, May 2007.

[3] M. F. A. Ahmed and S. A. Vorobyov, "Collaborative beamforming for wireless sensor networks with Gaussian distributed sensor nodes," *IEEE Trans. Wireless Commun.,* pp. 638-643, Feb. 2009.

[4] K. Zarifi, S. Affes, and A. Ghrayeb, "Distributed beamforming for wireless sensor networks with random node location," *ICASSP'09,* Taipei, Taiwan, Apr. 2009.

[5] B. Friedlander and B. Porat, "Performance analysis of a null-steering algorithm based on direction-of-arrival estimation," *IEEE Trans. Signal Process.,* vol. 37, pp. 461-466, Apr. 1989.

[6] B. D. Van Veen, "Minimum variance beamforming with soft response constraints," *IEEE Trans. Signal Process.,* vol. 39, pp. 1964-1972, Sep. 1991.

[7] L. C. Godara, "Application of antenna arrays to mobile communications, Part II: Beam-forming and direction-of-arrival considerations," *Proc. IEEE,* vol. 85, pp. 1195-1245, Aug. 1997.

[8] P. Gupta and P. R. Kumar, "Critical power for asymptotic connectivity in wireless networks," in *Stochastic Analysis, Control, Optimization and Applications: A Volume in Honor of W. H. Fleming,* W. M. McEneany, G. Yin, and Q. Zhang, Eds. Boston, MA: Birkhauser, 1998, pp. 547-566.

[9] M. Haenggi, "On distances in uniformly random networks," *IEEE Trans. Inf. Theory,* vol. 51, pp. 3584-3586, Oct. 2005.

[10] S. Mukherjee, D. Avidor, and K. Hartman, "Connectivity, power, and energy in a multihop cellular-packet system," *IEEE Trans. Veh. Technol.,* vol. 56, pp. 818-836, Mar. 2007.

[11] K. Zarifi, S. Affes, and A. Ghrayeb, "Collaborative null-steering beamforming for uniformly distributed wireless sensor networks," *IEEE Trans. Signal Process.,* to appear.

978-1-4244-4148-8/09/$25.00 ©2009
This full text paper was peer reviewed at the direction of IEEE Communications Society subject matter experts for publication in the IEEE "GLOBECOM" 2009 proceedings.